

# Discrete light propagation and self-trapping in liquid crystals

Andrea Fratolocchi and Gaetano Assanto

*NooEL-Nonlinear Optics and OptoElectronics Labs.  
Italian Institute for the Physics of Matter (INFM) and Dept. of Electronic Engineering, University "Roma Tre"  
Via della Vasca Navale 84, 00146 - Rome, Italy  
[Assanto@uniroma3.it](mailto:Assanto@uniroma3.it)*

[http://optow.ele.uniroma3.it/opto\\_2002.shtml](http://optow.ele.uniroma3.it/opto_2002.shtml)

Kasia A. Brzdąkiewicz and Mirek A. Karpierz

*Warsaw Univ. of Technology, Faculty of Physics  
Koszykowa 75, 00-662 Warsaw – Poland  
[Karpierz@if.pw.edu.pl](mailto:Karpierz@if.pw.edu.pl)*

**Abstract:** We investigate light propagation and self-localization in a voltage-controlled array of channel waveguides realized in undoped nematic liquid crystals. We report on discrete diffraction and solitons, as well as all-optical angular steering and the formation of multiband vector breathers. The results are in excellent agreement with both coupled mode theory and full numerical simulations.

©2005 Optical Society of America

**OCIS codes:** (190.0190) Nonlinear optics; (160.3710) Liquid crystals

---

## References and Links

1. S. Somekh, E. Garmire, A. Yariv, H. L. Garvin, and R. G. Hunsperger, "Channel optical waveguide directional couplers," *Appl. Phys. Lett.* **22**, 46-47 (1973).
2. S. M. Jensen, "The nonlinear coherent coupler," *IEEE J. Quantum Electron.* **QE-18**, 1580-1583 (1982).
3. N. Finlayson and G. I. Stegeman, "Spatial switching, instabilities, and chaos in a three-waveguide nonlinear directional coupler," *Appl. Phys. Lett.* **56**, 2276-2278 (1990).
4. C. Schmidt-Hattenberger, U. Trutschel, and F. Lederer, "Nonlinear switching in multiple-core couplers," *Opt. Lett.* **16**, 294-296 (1991).
5. S. Trillo and S. Wabnitz, "Coupling instability and power-induced switching with two-core dual-polarizations fiber nonlinear couplers," *J. Opt. Soc. Am. B* **5**, 483-491 (1985).
6. D. N. Christodoulides and R. I. Joseph, "Discrete self-focusing in nonlinear arrays of coupled waveguides," *Opt. Lett.* **13**, 794-796 (1988).
7. A. A. Sukhorukov, Y. S. Kivshar, H. S. Eisenberg, and Y. Silberberg, "Spatial optical solitons in waveguide arrays," *IEEE J. Quantum Electron.* **39**, 31-50 (2003).
8. H. S. Eisenberg, Y. Silberberg, R. Morandotti, and J. S. Aitchison, "Diffraction management," *Phys. Rev. Lett.* **85**, 1863-1866 (2000).
9. R. Morandotti, U. Peschel, J. S. Aitchison, H. S. Eisenberg, and Y. Silberberg, "Experimental observation of linear and nonlinear optical Bloch oscillations," *Phys. Rev. Lett.* **83**, 4756-4759 (1999).
10. D. Christodoulides, F. Lederer, and Y. Silberberg, "Discretizing light behaviour in linear and nonlinear waveguide lattices," *Nature* **424**, 817-823 (2003).
11. A. B. Aceves, C. de Angelis, T. Peschel, R. Muschall, F. Lederer, S. Trillo, and S. Wabnitz, "Discrete self-trapping, soliton interactions, and beam steering in nonlinear waveguide arrays," *Phys. Rev. E* **53**, 1172-1189 (1996).
12. M. Matsumoto, "Optical switching in nonlinear waveguide arrays with a longitudinally decreasing coupling coefficient," *Opt. Lett.* **20**, 1758-1760 (1995).
13. A. A. Sukhorukov and Y. S. Kivshar, "Generation and stability of discrete gap solitons," *Opt. Lett.* **28**, 2345-2347 (2003).
14. T. Peschel, R. Muschall, and F. Lederer, "Power-controlled beam steering in non equidistant arrays of nonlinear waveguides," *Opt. Comm.* **136**, 16-21 (1997).
15. D. N. Christodoulides and E. D. Eugenieva, "Blocking and routing discrete solitons in two-dimensional networks of nonlinear waveguide arrays," *Phys. Rev. Lett.* **87**, 233901 (2001).
16. T. Pertsch, U. Peschel, and F. Lederer, "All-optical switching in quadratically nonlinear waveguide arrays," *Opt. Lett.* **28**, 102-104 (2003).

17. O. Bang and P. D. Miller, "Exploiting discreteness for switching in waveguide arrays," *Opt. Lett.* **21**, 1105-1107 (1996).
18. T. Pertsch, T. Zentgraf, U. Peschel, A. Brauer, and F. Lederer, "Beam steering in waveguide arrays," *Appl. Phys. Lett.* **80**, 3247-3249 (2002).
19. W. Krolikowsky and Y. S. Kivshar, "Soliton-based optical switching in waveguide arrays," *J. Opt. Soc. Am. B* **13**, 876-880 (1996).
20. R. A. Vicencio, M. I. Molina, and Y. S. Kivshar, "Switching of discrete optical solitons in engineered waveguide arrays," *Phys. Rev. E* **70**, 026602 (2004).
21. N. K. Efremidis, J. Hudock, D. N. Christodoulides, J. W. Fleischer, O. Cohen, and M. Segev, "Two-dimensional optical lattice solitons," *Phys. Rev. Lett.* **91**, 213906 (2003).
22. A. A. Sukhorukov and Y. S. Kivshar, "Multigap discrete vector solitons," *Phys. Rev. Lett.* **91**, 113902 (2003).
23. O. Cohen, T. Schwartz, J. W. Fleischer, M. Segev, and D. N. Christodoulides, "Multiband Vector Lattice Solitons," *Phys. Rev. Lett.* **91**, 113901 (2003).
24. D. Mandelik, H. S. Eisenberg, Y. Silberberg, R. Morandotti, and J. S. Aitchison, "Observation of mutually trapped multiband optical breathers in waveguide arrays," *Phys. Rev. Lett.* **90**, 253902 (2003).
25. J. Hudock, P. G. Kevrekidis, B. A. Malomed and D. N. Christodoulides, "Discrete vector solitons in two-dimensional nonlinear waveguide arrays: solutions, stability, and dynamics," *Phys. Rev. E* **67**, 056618 (2003).
26. J. Meier, J. Hudock, D. Christodoulides, G. Stegeman, Y. Silberberg, R. Morandotti, and J. S. Aitchison, "Discrete vector solitons in Kerr nonlinear waveguide arrays," *Phys. Rev. Lett.* **91**, 143907 (2003).
27. D. Mandelik, H. S. Eisenberg, Y. Silberberg, R. Morandotti, and J. S. Aitchison, "Band-gap structure of waveguide arrays and excitation of Floquet-Bloch solitons," *Phys. Rev. Lett.* **90**, 053902 (2003).
28. R. Iwanow, R. Schiek, G. I. Stegeman, T. Pertsch, F. Lederer, Y. Min, and W. Sohler, "Observation of discrete quadratic solitons," *Phys. Rev. Lett.* **93**, 113902 (2004).
29. K. Sakoda, *Optical Properties of Photonic Crystals*, (Springer-Verlag, Berlin, 2001).
30. M. Peccianti, G. Assanto, A. de Luca, C. Umeton, and I. C. Khoo, "Electrically assisted self-confinement and waveguiding in planar nematic liquid crystal cells," *Appl. Phys. Lett.* **77**, 7-9 (2000).
31. M. Karpierz, "Solitary waves in liquid crystalline waveguides," *Phys. Rev. E* **66**, 036603 (2002).
32. G. Assanto and M. Peccianti, "Spatial solitons in nematic liquid crystals," *IEEE J. Quantum Electron.* **39**, 13-21 (2003).
33. C. Conti, M. Peccianti, and G. Assanto, "Observation of optical spatial solitons in a highly nonlocal medium," *Phys. Rev. Lett.* **92**, 113902 (2004).
34. M. Peccianti, C. Conti, G. Assanto, A. de Luca, and C. Umeton, "All-optical switching and logic gating with spatial solitons in liquid crystals," *Appl. Phys. Lett.* **81**, 3335-3337 (2002).
35. M. Peccianti and G. Assanto, "Signal readdressing by steering of spatial solitons in bulk nematic liquid crystals," *Opt. Lett.* **26**, 1690-1692 (2002).
36. A. Fratolocci, G. Assanto, K. A. Brzdańkiewicz, and M. A. Karpierz, "Discrete propagation and spatial solitons in nematic liquid crystals," *Opt. Lett.* **29**, 1530-1532 (2004).
37. I. C. Khoo, *Liquid crystals: physical properties and optical phenomena* (Wiley & Sons, New York, 1995).
38. D. A. Dumm, A. Fukuda, and G. R. Luckhurst, *Physical properties of liquid crystals: nematics* (INSPEC, London, 2001).

---

## 1. Introduction

Arrays of linear optical waveguides were firstly investigated in the early 1970's by Somekh *et al.*, who experimentally demonstrated light tunneling between neighboring channels [1]. This pioneering work paved the way to a number of nonlinear studies on the subject, concerning light propagation in a finite number of waveguides and exploiting discreteness to achieve all-optical switching [2-5]. A natural extension of those concepts is an infinite array of nonlinear identical channel waveguides, introduced by Christodoulides *et al.* in the late 1980's [6] and extensively analyzed in various materials and for diverse nonlinearities [7-28]. While the system dynamics becomes ungovernable when the number of optical channels exceeds three, a scheme with an infinite number of waveguides possesses a sufficient number of conservation laws which prevent chaotic instabilities and therefore allow to manage its properties [11]. Such periodic media can be simply described on the basis of coupled mode theory (CMT), which models light propagation as a superposition of guided-modes in channel waveguides coupled to their nearest-neighbors [6]. Light diffraction is therefore governed by the coupling between adjacent channels and the formation of discrete solitons –i.e., self-localized states in the lattice- can be intuitively pictured as resulting from the interplay between linear tunneling and nonlinear detuning. The refractive index increase arising from nonlinear self-focusing, in fact, mismatches nearby waveguides and reduces energy transfer

between propagating modes, favoring light localization in one or a few guides. To excite a discrete soliton, the input beam needs to detune a finite number of waveguides from the remaining of the array. In this case, the in-coupled light does not sense the presence of neighboring channels and can propagate without spreading. Since such detuning requires a lower power than the all-optical creation of a waveguide in a 1D bulk, the threshold to observe light localization in discrete media is usually lower than in their continuous counterparts. Furthermore, the rotational asymmetry of the system features interesting properties which can be exploited for all-optical switching devices [11,12,14-20]. Among them, the lack of self-localized "walking" solutions (narrow discrete solitons propagating at an angle through the lattice) leads to angular steering of a light beam: at low powers it can propagate obliquely with various degrees (or zero) of (discrete) diffraction, whereas in the nonlinear regime it excites a transversely immobile discrete soliton and the input energy is forced to flow straight along the confining (and decoupled from the rest) channels, regardless of the launching angle. This opens the possibility to all-optically routing of the emerging beam, with application to all-optical switching and multiport signal readdressing. [17,19]

When dealing with a 1D periodic array, the Floquet-Bloch mode expansion provides alternative and powerful insight on the spectrum of the array eigenmodes: it shows linear bands separated by gaps in which freely propagating modes do not exist [27,29]. Each gap support nonlinear localized states known as spatial "gap solitons", and interaction between modes gives rise to novel forms of vector multiband solitons and optical "breathers" [13,22-24,27].

Nematic liquid crystals (NLC) are optical materials with a giant non-resonant nonlinearity (orders of magnitude higher than conventional semiconductors), mature chemistry, physics and technology. This makes them ideal candidates to investigate nonlinear optics [30-33]. In addition, their large electro-optic response entails voltage-tunable architectures. NLC consist of elongated rod-like molecules which point towards an average direction in space, known as *director*, with a significant degree of orientational order. An external electric field (either static, or radio-frequency or optical) induces dipoles and tends to realign the NLC molecules with major axes parallel to its direction of oscillation (or polarization) in order to minimize the system energy. Although molecular reorientation is slow compared to electronic nonlinearities, the power level required to produce self-focusing is usually low (typically mW or less) and, therefore, quite amenable to all-optical switching in network reconfiguration applications (where bandwidth is not the crucial issue) [34-35].

In this Paper, after a brief summary of the basic model and sample geometry in Section 2, we illustrate the use of undoped nematic liquid crystals in discrete arrays of bias-tunable waveguides, and demonstrate discrete diffraction as well as discrete solitons and power-dependent steering in angle in Section 3. Taking advantage of the 1D periodic geometry encompassing a one-dimensional photonic crystal, we also demonstrate novel multiband breathers and their voltage-control in Section 4.

## 2. Sample and model equations

Our sample is sketched in Fig. 1 (left panel). A thin film of nematic liquid crystals -of thickness  $d$ - is sandwiched between two glass plates, which provide planar anchoring in the direction of light propagation. The plates are coated with an equally-spaced array of parallel Indium Tin Oxide (ITO) electrodes which, through the electro-optic response of the medium, allow to defining a set of identical channel waveguides supporting quasi-TM guided modes. [36] A bias  $V$ , in fact, corresponds to an electric field distribution which reorients the director in the  $(x,z)$  plane, yielding a refractive index modulation of period  $\Lambda$  across the sample. A typical index distribution is displayed in Fig. 1 (right panel).

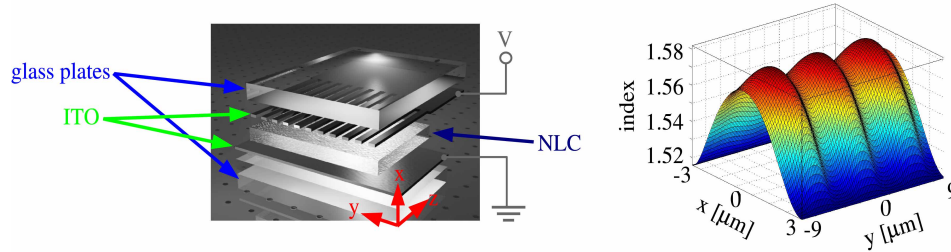


Fig.1. Left) Sketch of the NLC waveguide array. Right) Typical transverse index distribution for a bias of 1V.

A quasi-TM mode, with electric field polarized along  $x$ , experiences a refractive index  $n_e = n_{//}n_{\perp}(n_{//}^2 \cos^2 \theta + n_{\perp}^2 \sin^2 \theta)^{-1/2}$ , which depends on the mean angular molecular orientation  $\theta$  between the (propagation) axis  $z$  and the major molecular axis or director (subscripts  $//$  and  $\perp$  refer to field polarizations parallel or normal to the director, respectively). The steady-state director distribution can be calculated with the Frank free-energy formulation, [37-38] evaluating the NLC energy density and its minimum through the Euler-Lagrange equation:

$$K\nabla_{\perp}^2 \theta + \frac{\Delta \varepsilon_{RF} |E_x|^2}{2} \sin 2\theta = 0 \quad (1)$$

being  $E_x$  the  $x$ - component of the static or low-frequency field,  $K$  the elastic constant (single constant approximation [37]) and  $\Delta \varepsilon_{RF}$  the low-frequency birefringence. Maxwell equations are used to obtain the potential distribution  $V(x,y)$ :

$$\frac{\partial}{\partial x} \left[ (\varepsilon_{\perp} \cos^2 \theta + \varepsilon_{//} \sin^2 \theta) \frac{\partial}{\partial x} V \right] + \varepsilon_{\perp} \frac{\partial^2}{\partial y^2} V = 0 \quad (2)$$

Equations (1)-(2) can be solved numerically to analyze (or design) the array response. To the latter extent, we make use of the Floquet-Bloch (FB) mode expansion which, widely adopted in the field of photonic crystals, keeps into account all the modes and is not limited (as it is CMT) to the guided-modes of the single waveguides. Each FB eigenwave takes the form:

$$E_{FB} = \Pi_k(x, y) \exp j(k_y y - k_z z) \quad (3)$$

with  $k_y$  the Bloch wavenumber,  $k_z$  the propagation constant and  $\Pi(x,y)$  the beam envelope,  $\Lambda$ -periodic across  $y$ . By substituting Eq. (3) into Maxwell equations, we obtain:

$$\left[ \nabla_{\perp}^2 + 2jk_y \frac{\partial}{\partial y} + k_0^2 n^2(x, y) - k_y^2 \right] \Pi_k(x, y) = k_z^2 \Pi_k(x, y) \quad (4)$$

The eigenvalue problem (4) yields the band-gap spectrum ( $k_z$  as a function of  $k_y$ ) and the corresponding FB modes  $\Pi_k$ . The presence of the refractive index  $n(x,y)$  suggests that, in an electro-optic material such as NLC, the eigenvalue spectrum of the array can be adjusted through the external voltage. To demonstrate this peculiar feature, we numerically solved Eq. (4) with (1)-(2) in the bias range  $0.7 < V < 2.0V$  for a cell with  $\Lambda = d = 6\mu\text{m}$ , and show the results in Fig. 2. The band-gap spectrum (Fig. 2, left) consists of permitted bands (color lines), separated by gaps in which propagating modes are forbidden. As the bias increases, the width of each band-gap changes, as well. More specifically, as the index modulation grows for  $V < 1.3V$  (Fig. 2, right), the gaps widen in the spectrum (Fig. 2, center) due to an increasing refractive contrast. Conversely, for  $V > 1.3V$  non locality intervenes by reducing the index difference in-between waveguides (Fig. 2, right), thereby lowering the index modulation and shrinking the gaps once again. Discrete solitons (next section) appear above the first linear

band (band 0), while spatial gap-solitons exist in each of the lower gaps. [13, 27] Quite interestingly, light localization can also be originated by a proper superposition of linear FB modes, as shown in the last section.

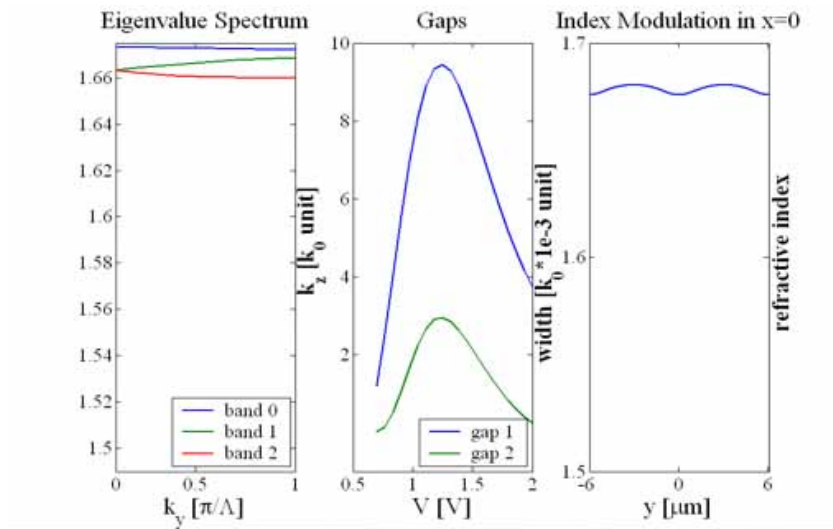


Fig. 2. (1123 KB) Eigenvalue spectrum of the array (left), width of first and second gaps (center) and corresponding refractive index (cross sections at the center of the cell,  $x=0$ ) for different biases. (Right) Gap 1 and gap 2 are between bands 0-1 and bands 1-2, respectively.

### 3. Discrete light localization in NLC

#### 3.1 Discrete solitons

We carried on experiments with a near infrared ( $\lambda=1.064\mu\text{m}$ ) Nd:YAG laser, collecting the light scattered out of the plane ( $y,z$ ) by a high resolution CCD. Results from a sample with  $\Lambda=8\mu\text{m}$  and thickness  $d=6\mu\text{m}$  are displayed in Fig. 3. At low launch-power ( $P=1\text{mW}$ ), when a single channel is excited, light couples from waveguide to waveguide and gives rise to the characteristic pattern of discrete diffraction (Fig. 3(a)). By varying the bias in the range  $0.65<V<1\text{V}$  while keeping constant the input power  $P=1\text{mW}$ , we monitored the beam evolution in the two cross sections at  $z_0=1.4\text{mm}$  and  $z_1=1.5\text{mm}$  (Fig. 3(b)). As the index modulation grows versus voltage, light experiences continuous ( $V<0.7\text{V}$ ) or discrete diffraction ( $V>0.7\text{V}$ ). In the latter regime the coupling distance (i.e., the coherence length of each two-channel directional coupler) increases with the bias, because of the improved confinement afforded by each channels. Conversely, if the input power grows for a given bias  $V=0.74\text{V}$  (Fig. 3(c)), the all-optical increase in refractive index detunes the excited waveguide. Figure 3(c) shows light evolution in versus power in  $1.40<z<1.55\text{mm}$ . Eventually, when the excitation is large enough ( $P=10\text{mW}$ ), light gets completely trapped in one waveguide and a discrete soliton is generated in the array, as visible in Fig. 3(d).

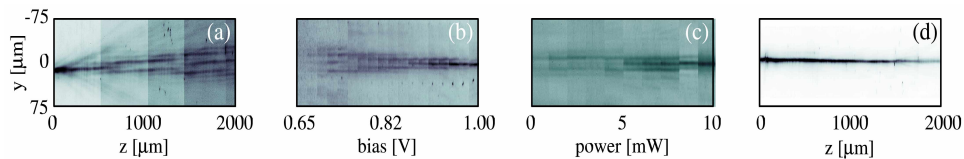


Fig. 3. Experimental response of the NLC array with  $\Lambda=8\mu\text{m}$ : (a) discrete diffraction in ( $y,z$ ) for  $P=1\text{mW}$ ; (b) assembled photographs of light propagation in  $z_0<z<z_1$  versus bias and (c) versus input power; (d) photograph of a discrete soliton excited by  $P=10\text{mW}$  and propagating along the input channel.

A comparison with the theory is performed in Fig. 4, which shows discrete soliton generation as predicted by simulations with a nonlinear beam propagator (BPM). To the latter extent, we added the term  $\varepsilon_0(n_{//}^2 - n_{\perp}^2)E_x^{AC}|\sin 2\theta/4$  to Eq. (1), with  $E_x^{AC}$  the beam envelope at optical frequency. Coupled-mode theory, in fact, does not keep into account the non-local response of NLC, hence and a more accurate tool is needed. Since power coupling efficiency into each channel is unknown and could not be evaluated in our sample, the response in Fig. 4 is in excellent agreement with the experimental data (Fig. 3).

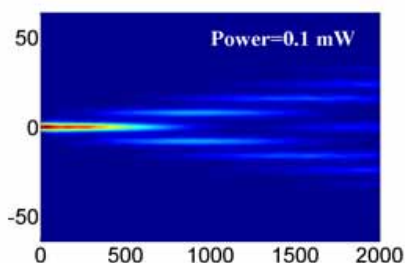


Fig. 4. (222 KB) Animation showing light propagation in the plane  $(y,z)$ , evolving from diffraction to discrete soliton generation as the power injected in a single channel ramps from 0.1 to 1.0 mW. Here  $V=0.74$  V ( $z$ - and  $y$ -axes units are in  $\mu\text{m}$ ).

### 3.2 Discrete Beam steering

Discrete beam steering has been theoretically investigated in the past few years. [11,17,19] It can be simply understood on the basis of coupled mode theory, and analyzed with reference to our material system by BPM simulations, as in Fig. 5. A Gaussian beam ( $w_y=10\mu\text{m}$ ) impinges on the waveguide array ( $A=8\mu\text{m}$ ,  $V=0.77$  V) with an input tilt  $\gamma=\lambda/4A=1.90^\circ$  along  $y$  as to excite the array at maximum transverse velocity and minimum diffraction. [8] In the linear regime ( $P=P_L=0.1\text{mW}$ ), light couples between adjacent waveguides and "walks" across the array (Fig. 5(a)), as also expected based on CMT. As the power increases, the nonlinear detuning of the central waveguide (i.e., the one excited by the peak beam intensity) at sufficiently high power ( $P=P_H=2\text{mW}$ ) causes light trapping and the excitation of a discrete soliton, which is forced to propagate straight along the input channel, as in Fig. 5(b). After propagating over  $z=2\text{mm}$ , the input beam in the two cases displays a significant lateral shift as the power changes from  $P_L$  to  $P_H$ , as graphed in Fig. 5(c).

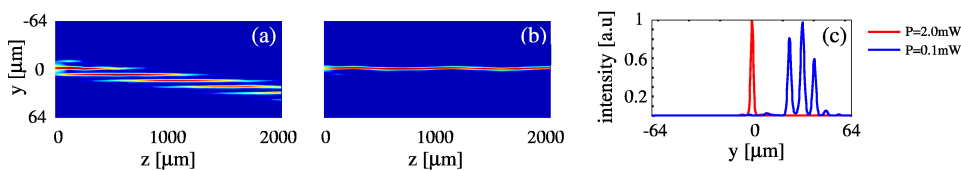


Fig. 5. BPM simulations of discrete beam steering: (a) linear ( $P_L=0.1\text{mW}$ ) and (b) nonlinear ( $P_H=2.0\text{mW}$ ) light propagation in  $(y,z)$ ; (c) corresponding cross-section of the output intensity distribution in  $z=2\text{mm}$ .

Such predictions were verified in our experiments, as summarized by Fig. 6 for a Gaussian input of waist  $w_y=10\mu\text{m}$  and an array with  $A=8\mu\text{m}$  and  $V=0.77$  V. Light discretely diffracts for a low power  $P=P_L=1\text{mW}$  (Fig. 6(a)), and localizes in a single channel when the power reaches  $P=P_H=7\text{mW}$  (Fig. 6(b)). The intensity cross-sections in  $z=2\text{mm}$  clearly show nonlinear beam steering (Fig. 6(c)).

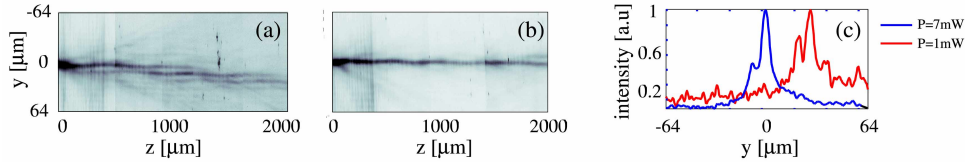


Fig. 6. Experimental observations of angular beam steering: (a) discrete diffraction of a tilted beam for  $P_L=1\text{mW}$ ; (b) observation of nonlinear steering for  $P_H=7\text{mW}$ ; (c) profiles of the output intensity in  $z=2\text{mm}$ .

The device, being able to all-optically “steer” a confined signal, has potential applications in all-optical switching and multiport routing schemes. The output location (i.e., the output waveguide in the array) of a light signal can be controlled by varying the input power. Our experiments enlighten the advantages of NLC in terms of low-power requirements, low voltage ( $V<1\text{V}$ ) and device compactness ( $L<2\text{mm}$ ). Array optimization (beyond the scope of this paper) would rely on the reduction of period  $\Lambda$  (decreasing device length because of a higher overlap between evanescent fields) and the minimization of propagation losses (mostly due to scattering with a  $1/\lambda^2$  dependence in NLC) by operating at longer wavelengths. [37]

#### 4. Multiband vector breathers

A multiband optical breather originates from the vectorial superposition of modes belonging to different band-gaps and, therefore, characterized by slightly different propagation constants. While each of the individual modes would linearly diffract or nonlinearly self-localize if individually excited, their simultaneous presence can give rise to a longitudinally oscillating, transversely localized, discrete beam via cross-phase modulation. Due to its binary composition, in fact, such solitary wave periodically oscillates or “breathes” in propagation. [24] In vector breathers, as investigated here, none of the input modes is able to self-trap. Their formation can be predicted by BPM simulations (see Fig. 7) by exciting superimposed FB modes belonging to different bands. FB modes of band 0 possess amplitude maxima in the waveguide-core regions (Fig. 7(a), top), and can be excited by a wide Gaussian beam (of waist  $w_y=8\mu\text{m}$  across  $y$ ) launched on-axis and equidistant from two neighboring channels. In this case, light propagation for  $P=0.2\text{mW}$  (Fig. 7(b), top) exhibits a pattern characteristic of discrete diffraction. Modes of band 1, conversely, are characterized by maxima between channels (Fig. 7(a), bottom) and can be excited by a narrow Gaussian input centered between two adjacent waveguides (Fig. 7(b), bottom). When co-launched with a total power of  $P=0.4\text{mW}$ , the previous FB modes originate a symmetric breather, oscillating in a periodic fashion as it propagates along  $z$  (Fig. 7(c)).

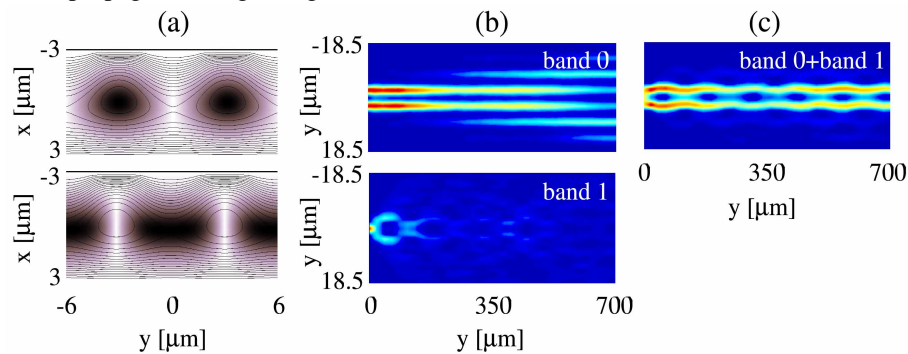


Fig. 7. Numerical (BPM) experiments on vectors breather in NLC: (a) Floquet-Bloch profiles (density plots) with corresponding refractive index distributions for  $V=1\text{V}$  (contour lines) and  $k_y=1$  in band 0 (top) and band 1 (bottom); (b) light propagation of FB modes belonging to band 0 (top) and band 1 (bottom) for  $P=0.2\text{mW}$ ; (c) a vector breather generated by superimposing band 0 and band 1 excitations (b) with a total  $P=0.4\text{mW}$ .

Using the setup previously employed to demonstrate discrete solitons and their steering, we carried out experiments on an array with  $\Lambda=d=6\mu\text{m}$ . Fig. 8 displays our results. To ensure an adequate spatial overlap with modes of the first two bands, we used a single Gaussian beam of waist  $w_y=5\mu\text{m}$  centered between neighboring waveguides. In this configuration, the spatial overlap is larger between the input and modes in band 1, because the intensity peaks between channels. At low power ( $P=0.2\text{mW}$ ), in fact, we observed light spreading across the array (Fig. 8(a)) as in the numerical experiment of Fig. 7(b), bottom panel. At high power ( $P=7\text{mW}$ ), a symmetric breather is formed via cross phase modulation and propagates in the array (Fig. 8(b)). The beating and its period depend on the slight difference between the propagation constants of the sourcing FB modes. Since their position in the dispersion diagram can be electro-optically adjusted, we expected to be able to tune such period by varying the applied bias, i.e., by altering the width of gap 1. The calculated gap-width and the measured breathing period are graphed in Fig. 8(c) versus applied voltage. Clearly, as the width of gap 1 has a maximum in  $V=1.3\text{V}$  (red line), correspondingly the period exhibits a minimum around the same value (blue dots). As  $V>1.3\text{V}$ , non locality of NLC mediates reorientation between neighboring channels, shrinking the gap and lengthening the period once again.

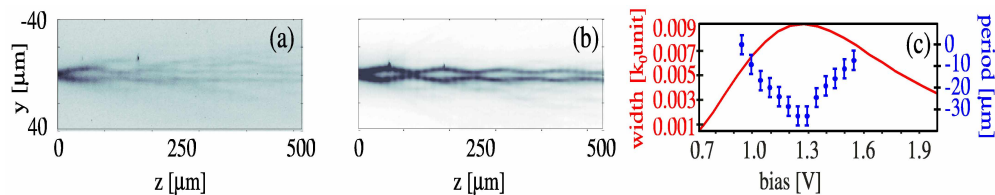


Fig. 8. (a) Low power  $P=0.2\text{mW}$  and (b) high power  $P=7\text{mW}$  light propagation in the NLC array excited by a Gaussian beam with  $w_y=5\mu\text{m}$  launched between waveguides. (c) Breather period (blue dots and error bars) and calculated width of gap 1 (red solid line) versus applied bias.

## 5. Conclusions

We have investigated various self-localization phenomena in a voltage-controlled array of channel waveguides realized in undoped nematic liquid crystals. Discrete solitons, breathers and discrete angular steering were demonstrated in the near infrared, in excellent agreement with models based on physical and geometric parameters. The NLC array proved to be an efficiently tunable 1D photonic crystal, an outstanding workbench to study optical propagation in a discrete system and a good candidate for the realization of compact, low power and broadband all-optical switches.